ARTICLE - Plasma Cell Disorders

IL6Myc mouse is an immunocompetent model for the development of aggressive multiple myeloma

Michael D. Pisano,[1,2] Fumou Sun,[3] Yan Cheng,[3] Deepak Parashar,[2] Vivian Zhou,[2] Xuefang Jing,[4] Ramakrishna Sompallae,[5] Jenica Abrudan,[6] Michael T. Zimmermann,[6] Angela Mathison,[6] Siegfried Janz[2] and Miles A. Pufall[7]

[1]Interdisciplinary Graduate Program in Immunology, University of Iowa, Iowa City, IA; [2]Division of Hematology and Oncology, Department of Medicine, Medical College of Wisconsin, Milwaukee, WI; [3]Myeloma Center, Department of Internal Medicine and Winthrop P. Rockefeller Cancer Institute, University of Arkansas for Medical Sciences, Little Rock, AR; [4]Department of Pathology, University of Iowa Roy J. and Lucille A. Carver College of Medicine, Iowa City, IA; [5]Iowa Institute for Genetics, University of Iowa Roy J. and Lucille A. Carver College of Medicine, Iowa City, IA; [6]Genomic Sciences and Precision Medicine Center, Medical College of Wisconsin, Milwaukee, WI and [7]Department of Biochemistry and Molecular Biology, the University of Iowa Roy J. and Lucille A. Carver College of Medicine, Holden Comprehensive Cancer Center, Iowa City, IA, USA

Correspondence: M.A. Pufall
mpufall@uiowa.edu

Received: December 12, 2022.
Accepted: July 4, 2023.
Early view: July 13, 2023.

https://doi.org/10.3324/haematol.2022.282538

Supplemental Materials

IL6Myc mouse is an immunocompetent model for the development of aggressive multiple myeloma

Michael D Pisano[1,2], Fumou Sun[3], Yan Cheng[3], Deepak Parashar[2], Vivian Zhou[2], Xuefang Jing[4], Ramakrishna Sompallae[5], Jenica Abrudan[6], Michael T Zimmermann[6], Angela Mathison[6], Siegfried Janz[2], Miles A Pufall[7]

Supplemental File

An excel spreadsheet (IL6Myc_v_activated_b_DGE.xlsx) containing differential expression values and statistics for IL6Myc tumor versus normal B cell controls measured by RNA-seq and reverse phase protein arrays (RPPAs) is available online. Methods for processing these data are describe below.

Supplemental Figures

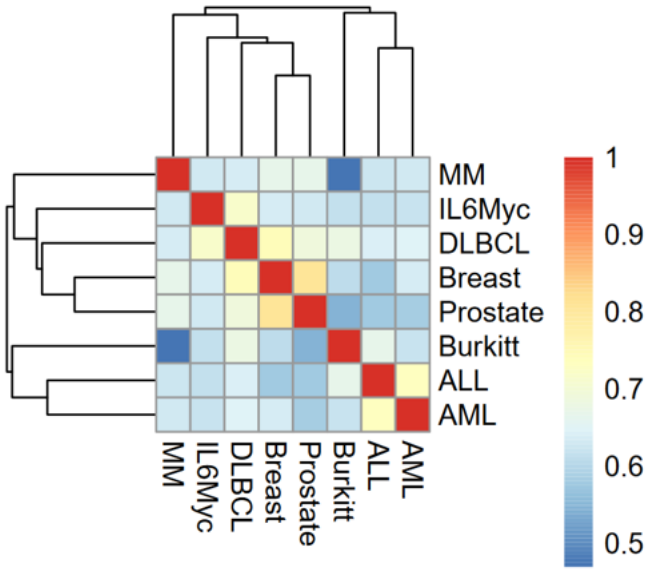

Figure S1. Hierarchical Clustering of IL6Myc tumor and Human Malignancies Heatmap showing the pairwise correlations of tumor profiles for pathway enrichment scores and hierarchical clustering using single linkage method.

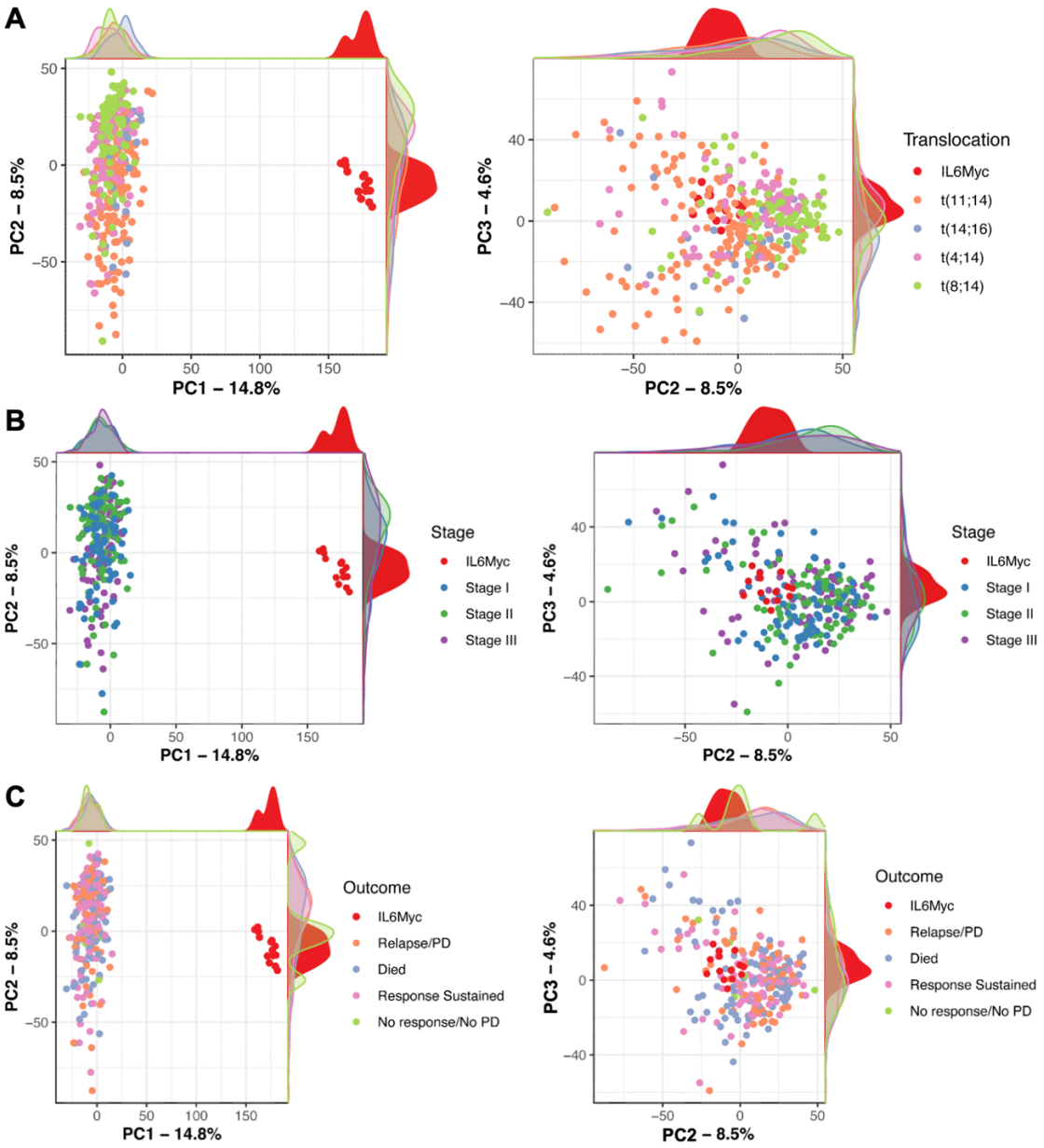

Figure S2. Grouping of IL6Myc with MMRF Samples by Disease Stage and Outcome A) PCA of IL6Myc cell lines compared to the MMRF dataset with grouping examined by disease stage when the sample was taken. **B)** PCA of Il6Myc cell lines compared to the MMRF dataset with grouping examined by outcome in the MMRF study.

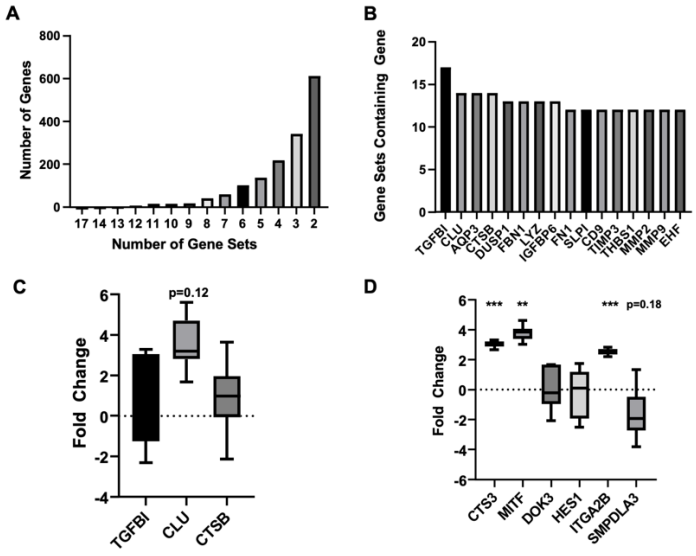

Figure S3. Validation of Leading Edge Genes Confirms IL6Myc Resemblance to the MS Subset of Human MM A) Summary data of how many genes that were found in the leading edge of multiple gene sets (2-17 gene sets). **B)** The top 15 genes most commonly found in the leading edge of the top 100 most enriched gene sets. **C)** qPCR data suggesting modest fold increases in expression of TGFBI and CTSB in IL6Myc and moderate fold change expression of CLU. **D)** qPCR validation of Myeloma Associated Gene Sets. Significance of <0.01 indicated by ** and <0.001 indicated by ***.

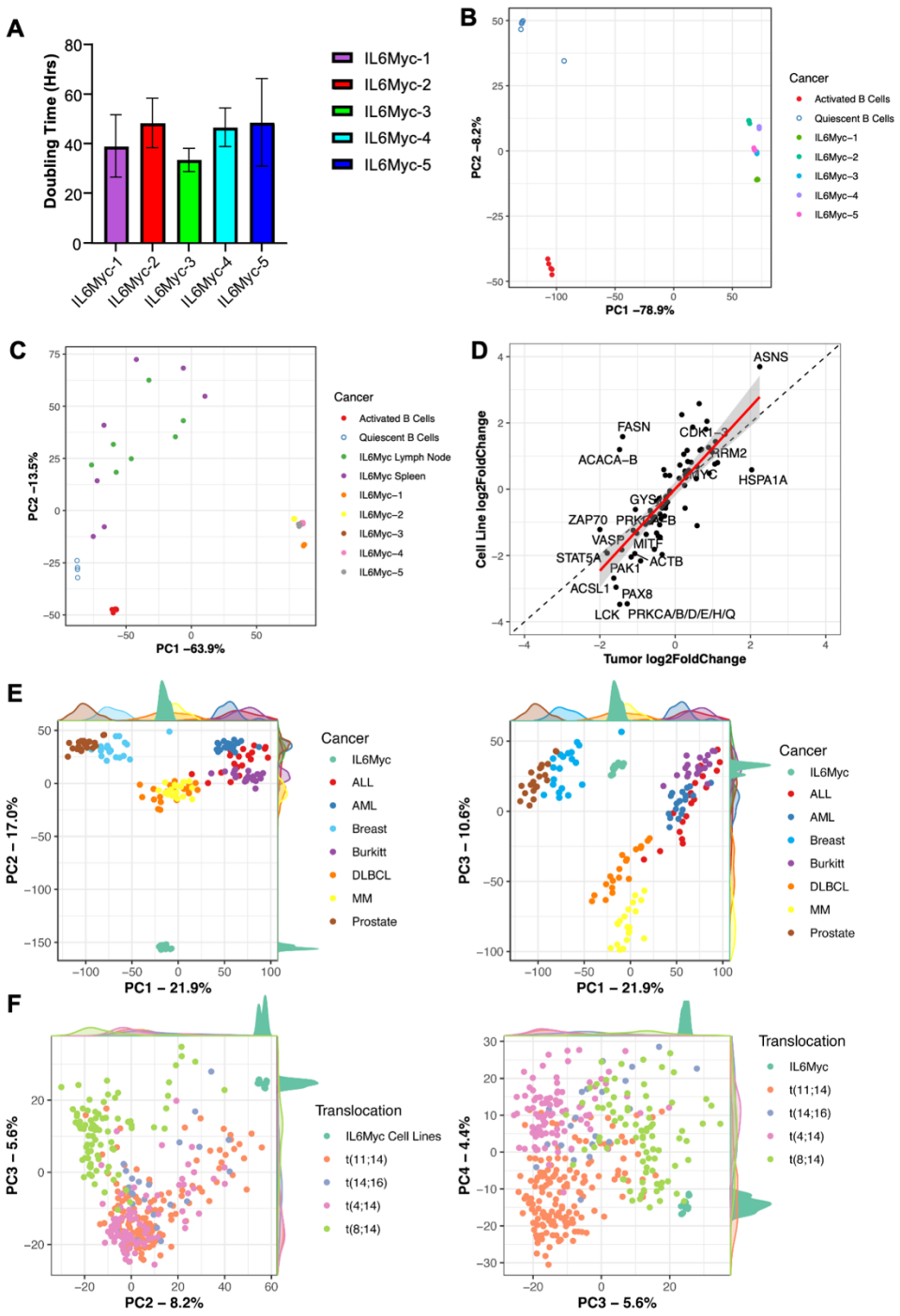

Figure S4. IL6Myc Cell Lines Cluster Best with Human Multiple Myeloma but not a Specific Subtype. A) Doubling times of IL6Myc cell lines. **B)** PCA of IL6Myc cell lines. Individual dots indicate biological replicants. **C)** PCA of IL6Myc primary tumor and IL6Myc cell lines **D)** Comparison of log2FoldChange in protein expression for IL6Myc tumors (x axis) versus Il6Myc cell lines (y axis) generated by RPPA compared to wild type B cells. **E)** PCA of IL6Myc Cell Lines Compared to Several Human Malignancies. Data downloaded from TCGA. PC2 is excluded (right) due to distinguishing human and mouse samples. Red circles indicate the

group of IL6Myc cell lines. **F)** PCA of IL6Myc Cell Lines Compared to Human MM from the MMRF CoMMpass Database. Red circles indicate the group of IL6Myc cell lines.

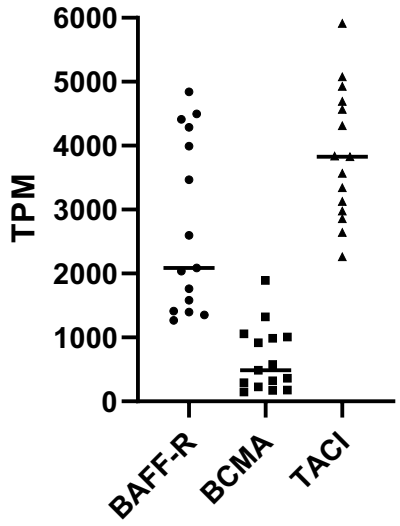

Figure S5. RNA-seq expression levels of BAFF-R, BCMA, and TACI. RNA-seq of five IL6Myc cell lines was performed, and count tables were converted to transcripts per million (TPM) for comparison. TPM levels indicate that BCMA RNA is expressed at a reasonable level (~500 TPM) in these cell lines, despite a lack of detection of the protein on the cell surface. Expression of BAFF-R and TACI are considerably higher, which is reflected in the positive cell surface staining.

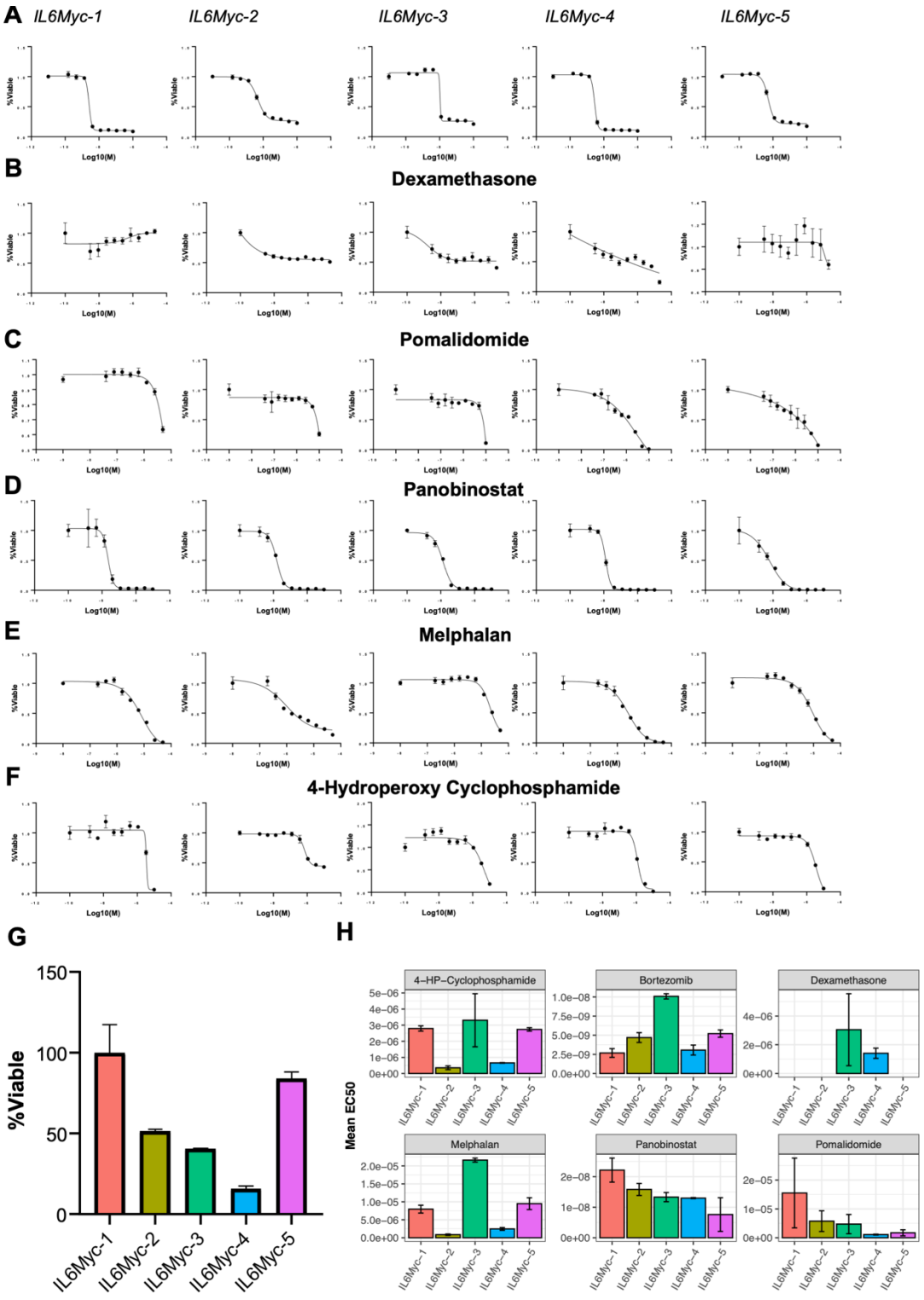

Figure S6. Sensitivity of IL6Myc cell lines to pharmacological agents commonly used in multiple myeloma. Five cell lines (IL6Myc-1:5) were tested. **A)** Viability of cell lines after treatment with dilutions (Starting at 1 μM, 1:3 dilutions) of bortezomib for 24 hrs. **B)** Viability of cell lines after treatment with dilutions (Starting at 10 μM, 1:3 dilutions) of dexamethasone for 72 hrs. **C)** Viability of cell lines after treatment with dilutions (Starting at 10 μM, 1:2 dilutions) of

pomalidomide for 72 hrs. **D)** Viability of cell lines after treatment with dilutions (Starting at 10 μM, 1:3 dilutions) of panobinostat for 72 hrs. **E)** Viability of cell lines after treatment with dilutions (Starting at 50 μM, 1:2 dilutions) of melphalan for 72 hrs. **F)** Viability of cell lines after treatment with dilutions (Starting at 10 μM, 1:3 dilutions) of 4-hydroperoxy cyclophosphamide for 24 hrs. **G)** Viability of IL6Myc cell lines after incubation with 10 μM dexamethasone after 72hrs. **H)** Summary of EC50 Values of bortezomib, 4-hydroxyperoxy cyclophosphamide, dexamethasone, melphalan, panobinostat and pomalidomide. Viability was normalized to 100% using wells with vehicle control, curves were fit with GraphPad Prism, EC50s were calculated in R, and error bars represent the standard deviation.

Supplemental Methods

Mice: IL6Myc mice were bred by crossing C.IL6 and iMyc$^{E\mu}$ mice as described in our 2010 publication first describing this model.[13] All mice are on a BALB/c background and were already contained in our mouse colony. All animal studies were conducted under the Medical College of Wisconsin Animal Use Application: AUA00006541 Mice were from a variety of tumor bearing ages. Exact ages are shown below:

Mouse Identification #	Age (Days)
1609	163
1610	120
1611	122
1612	201
1613	147
1614	158
1615	147
1616	147

B cell collection for RNA-sequencing: Seven IL6Myc splenic and MLN tumor and 9 WT spleen were isolated from mice and then processed by being blended through a 70 μm cell strainer. Red blood cells were then lysed from the blended tissue using 1X RBC Lysis Buffer (eBioscience, 00-4333-57) and washed twice with PBS containing 2% FBS. Cells were resuspended in 2% FBS PBS and were selected via MACS sort using the untouched B Cell Isolation Kit (Miltenyi Biotec, 130-090-862). The effectiveness of the untouched b cell sort was confirmed by flow cytometry detection of >90% B220 (BD Pharmingen, 553088) and CD138 (BD Pharmingen, 553714). B cells from WT spleen were divided into two groups for use as controls: 5 activated and 4 quiescent. Activated B cells were generated by culture with 1ug/ml LPS for 16 hours prior to RNA extraction. This phenotype was confirmed using flow cytometry detection of B220 and CD138.

RNA sequencing of Primary IL6Myc Tumor: RNA was extracted using the RNeasy mini kit (Qiagen, 74106). RNA quantity and quality was confirmed using the Thermofisher Nanodrop machine and Agilent 2100 machines. Samples were sequenced using 150 Paired-end (PE) runs on the Illumina NovaSeq 6000 system. Bioinformatics analysis of RNA sequencing data was conducted in R-Studio 4.1.1 and was done as follows. TrimGalore! was used to trim adapters of the RNA-seq library and then the data was mapped to GENCODE VM27 GTF file from the GRCm39 assembly with Salmon version 1.5.1. Differential expression testing was performed using the DESeq2 package which allowed extraction of TPM, FPKM, and RPKM data for downstream analysis. Figures were plotted using ggplot2 in R-Studio 4.1.1. Knitted R scripts are included as additional supplemental documents.

Gene Set Enrichment Analysis (GSEA): Gene set enrichment analysis was conducted using TPM data from IL6Myc tumor (n=14) which was compared to TPM data from activated WT B cells (n=5). TPM data was generated during the RNA sequencing analysis described above. Analysis was conducted using the UC San Diego and Broad Institute GSEA analysis tool downloadable at http://www.gsea-msigdb.org/gsea/index.jsp. Significant gene sets were determined using a FDR cut off of 10% and nominal P of >.01. Top gene sets were ranked by normalized enrichment score (NES) and gene sets of interest were selected from the top 100

gene sets. To validate key genes qPCR was performed in two independent steps using the iScript™ cDNA Synthesis Kit (Bio-Rad) and SYBR® Green Master Mix (Bio-Rad) according to manufacturer guidelines.

Comparison of Mouse and Human RNA-seq: To compare gene expression of mouse IL6Myc tumors to human tumors, we compared our FPKM data from IL6Myc to FPKM tables for 25 samples each for AML, ALL, Burkitt's Lymphoma, DLBCL, lung, and prostate cancer (The Cancer Genome Atlas (TCGA)). Human MM RNA-seq data was downloaded from the MMRF CoMMpass portal at https://research.themm rf.org. TPM and FPKM spreadsheets were downloaded from the "downloads" tab and demographic information was matched manually with the demographic spreadsheet in this tab. For comparisons of IL6Myc and human fusion genes a filtered list of MMRF gene fusions was downloaded from the supplemental files of PMID: 324719901[4].

Data was processed using DESeq2 and tidyverse and PCAs were plotted using ggplot2 in RStudio 4.1.1. PCAs were plotted using ggplot2. R script is included as supplementary materials.

Tumor similarity using functional pathways: To compare the expression profiles of different tumor types with a set of functional pathways, the gene set enrichment analysis (GSEA)[1] was performed using the R software package, fast gene set enrichment analysis (fgsea)[2]. Curated gene sets of 3050 human pathways were obtained from MSigDB resource[3]. First, the mean FPKM values were computed as stable expression profile for each tumor type. The mean expression profiles were than transformed into pathway enrichment scores. Next, the tumor types were clustered using the correlation of adjusted p-values from pathway enrichment.

Reverse-phase proteomic array (RPPA): Forty-five IL6Myc MLN tumor samples and activated 3 WT Balb/c isolated B cells were submitted to MD Anderson as two separate experiments. Protein was extracted using RPPA lysis buffer by the MD Anderson RPPA core. Forty-four of forty-five tumor samples passed quality control. The 44 MLN tumor samples and 3 WT B Balb/c isolated B cells were run on RPPA set 154 and 191 respectively and were probed with 361 and 488 antibodies respectively. The list of antibodies can be found at: https://www.mdanderson.org/research/research-resources/core-facilities/functional-proteomics-rppa-core/antibody-information-and-protocols.html. Downstream analysis was conducted on the 333 antibody targets which were shared between the two experiments. Level 4 data was used to compare data from WT Balb/c isolated B cells and IL6Myc MLN tumor and data was analyzed using GraphPad Prism and Ingenuity Pathway Analysis (IPA). Significantly differentially regulated proteins were determined by using multiple T-test comparisons.

Whole exome sequencing (WES): Forty-five IL6Myc MLN tumor samples and five BALB/c Kidney samples were processed for WES. Kidney was included as control tissue. DNA was extracted whole tumor using the DNeasy mini kit (Qiagen, 69506). Quality and quantity of DNA were measured using the Thermofisher nanodrop machine and samples were shipped to BGI genomics for sequencing and library preparation. The WES library was constructed using the SureSelectXT Mouse All Exon kit (Agilent, 5190-4642) and 150PE sequencing was performed on an Illumina HiSeq 4000 machine.

Sequencing of mouse whole exome regions and the preliminary analysis of read alignment to reference genome was performed at BGI. Mouse genome version, mm10 was used as the reference sequence. Somatic variants were called using Mutect2 program from the GATK

(Genome Analysis Tool Kit) software package (version 4.0.5.2) developed by the Broad Institute[5]. Mutect2 program was run in Tumor only mode. The common germline and other artifactual variants detected in normal samples were used as panel of normals (PoN) to filter variant calls from tumor samples. For each sample, variants with quality flag 'PASS' and the allele frequency greater than 5% were considered for further analysis. Mouse strain specific germline mutation calls were identified and filtered out using the variation data from Sanger Mouse Genomes Project (MGP). Somatic variant calls from all tumor samples were combined with sample columns indicating the variant allele frequencies. The Ensembl Variant Effect Predictor (VEP) software was used for variant annotation[6] to determine the effect of somatic variants. Variants were further filtered out based on the coding regions and the consequence of mutations. While mutations annotated as missense variant, splice-site mutations, stop gain, stop lost, frameshift deletions, frameshift insertions, in-frame deletions and in-frame insertions all other were excluded.

All canonical variants were downloaded from the downloads tab of the MMRF CoMMpass portal at https://research.themmrf.org/ and matched manually with the demographics spreadsheet found in this tab. The list was further filtered so that only exonic variants were considered for comparison with variants found in IL6Myc. In addition, silent mutations were filtered out leaving a list of variants with a predicted transcriptional effect. Overlap with a list of 80 known MM driver genes was determined from a list from the following publication: PMID: 33767199. Overlap between human and mouse WES datasets was determined using the Lund Lab's statistical significance of the overlap between two groups of genes program (http://nemates.org/MA/progs/overlap_stats.html). Number of genes in the genome was defined as 22,810 as this is the number of protein coding genes in Ensembl R74.

Isolation of IL6Myc Cell Lines: IL6Myc cell lines were derived from splenic (IL6Myc-1) and mesenteric lymph node (IL6Myc-2,3,4,5) tumor of tumor bearing IL6Myc mice. Tumor was processed by being blended through a 70 µm cell strainer. Red blood cells were then lysed from the blended tissue using 1X RBC Lysis Buffer (eBioscience, 00-4333-57) and washed twice with PBS containing 2% FBS. Cells were resuspended in 2% FBS PBS and malignant plasma cells were sorted via magnetic separation using the $CD138^+$ Plasma Cell Isolation Kit, mouse (Miltenyi, 130-092-530). Cells were then seeded as single cells in a 96 well plate and candidate cell lines were picked from surviving single clones. Candidate cell lines with poor growing efficiency (poor viability at confluence or slow doubling time) were abandoned leaving five independently derived cell lines. The ability of Il6Myc derived cell lines to survive and proliferate *in vitro* was then determined using the PrestoBlue™ Cell Viability Reagent (Invitrogen, A13261) according to manufacturer recommendations. From these values doubling times were calculated and compared for significant differences using a T-test.

***In vitro* culture of IL6Myc Derived Cell Lines:** Cell lines were cultured in IMDM (12440053, Gibco) supplemented with 15% heat inactivated (65°C, 30 min) fetal bovine serum and 1% v/v antibiotic/antimycotic solution (15240062, Gibco) under standard culture conditions (37°C, 5% CO2) in T25 flasks unless otherwise noted.

Adoptive transfer of IL6Myc-1 cells IL6Myc-1 cells were derived from the spleen of a PCT-bearing IL6Myc mouse. For Balb/c mice, 2×10^6 IL6Myc-1 cells were transferred IV to lethally irradiated mice rescued by co-transfer of hematopoietic stem cells obtained from untreated Balb/c mice. For NOD-SCID mice, 2×10^6 IL6Myc-1 cells were transfered to untreated NOD-

SCID mice. Tumor manifestation required ~3 months and ~3 weeks in Balb/c and NOD-SCID mice, respectively.

X-ray microscopy and µCT imaging Mouse carcasses, fixed in formalin and tightly fitted in 50-ml plastic tubes to prevent movement, were imaged ex vivo using dual-energy 3D X-ray microscopy (Zeiss Xradia 520 Versa). The scan was performed at 80 kV and reconstructed to a pixel size of 50 μm^2 or 8 μm^2. Projections were collected through 360° rotations. Three-dimensional (3D) parameters BV/TV (bone volume over tissue volume), Tb.Th (trabecular thickness) and Tb.Sp (inter-trabecular space) were analyzed with the help of the BoneJ (v. 1.3.14) plugin of ImageJ (v. 1.49 m). Ten 4-5 months old PCT-carrying transgenic mice (5 males and 5 females) were compared with 3 age-matched normal C mice (2 males and 1 female) used as control.

Histological analysis and TRAP staining Bone samples were fixed in formaldehyde, decalcified in 10% EDTA (6 days, 4 °C), rinsed with PBS, fixed in cold 70% ethanol, and embedded in paraffin. Tissue sections were deparaffinized and stained for tartrate-resistant acid phosphatase (TRAP) activity, using an acid phosphatase leukocyte kit from Sigma according to the manufacturer's suggestions. Specimens were counterstained with eosin and mounted for imaging and histomorphometry. Osteoclasts were enumerated in five high-power microscopy fields per slide. Five slides per specimen were evaluated.

Serum analysis At sacrifice of mice, ~1-ml blood was obtained by cardiac puncture and subjected to centrifugation to obtain a serum sample. Levels of RANKL and OPG were determined using ELISA according to the manufacturer's instructions (R&D Systems, Abingdon, UK). TRACP-5b was measured with the help of an ELISA kit from MyBioSource (San Diego, USA).

Flow Cytometry of IL6Myc Derived Cell Lines: $1x10^6$ cells were isolated from culture, spun down and washed with PBS. Next, the cells were resuspended in 50ul and blocked with 1ug Fc blocking antibody for 10min. Afterwards an additional 50ul containing antibodies at concentrations according to manufacturer recommendations was added and the samples were incubated in the dark at room temperature for 30min. These cells were then spun down and washed with PBS twice. Cells were resuspended in 300ul of PBS with 2% FBS and vortexed lightly prior to being run on a BD Accuri™ C6 Plus Flow Cytometer. The antibodies that were used are as follows: CD138(Biolegend, 142503), SLAM7(Biolegend, 152004), CD54(eBioscience, 12-0541-81), CD20(Biolegend, 152106), B220 (eBioscience, 12-0452-82), CD19 (BF Pharmingen, 553785), BCMA(Miltenyi Biotec, 130-108-327), TACI(eBioscience, 17-5942-81), BAFF-R(Biolegend, 134104), CD38(eBioscience, 11-0381-81), CD56(eBioscience, 17-0567-41), CD27(eBioscience, 17-0271-81), CD24(Biolegend, 101814), CD48(eBioscience, 25-0481-80), CD81(Invitrogen, MA5-17939), NKG2D(Biolegend, 320808), CD117(eBioscience, 12-1178-42). Samples were run with a limit of 50,000 events and data was analyzed using FlowJo Software.

BAFF and APRIL Stimulation of IL6Myc Cell Lines: Cells were harvested from culture and seeded in 100ul IMDM containing 1% FBS at a concentration of $1x10^5$ cells per well in a clear plastic flat bottom 96 well plate. Experimental groups were contained in one column each with a total of 8 replicates. Experimental groups were as follows: negative (1% FBS IMDM with no other additions), media containing 100ng/ml recombinant APRIL (Biovison, ab50096) and media containing 100ng/ml recombinant BAFF (AdipoGen Life Sciences, AG40B00223010). After

72hrs cells were cultured with 20ul of MTS reagent (MTS Cell Proliferation Colorimetric Assay Kit, Biovision) per well at 37 degrees for 45min. Plates were then read on the SpectraMax i3x (Molecular Devices) machine at a wavelength of 490nm. Significant differences were determined by T-test comparisons to the negative group.

Drug Testing and Viability of IL6Myc Derived Cell Lines: Cells were harvested from culture and seeded in 100ul of 15% FBS IMDM at a concentration of $1x10^5$ cells per well in a clear plastic flat bottom 96 well plate. 10ul of media containing a drug of interest was added at the proper concentration to each well. Drugs bortezomib, melphalan, 4-hydroperoxy cyclophosphamide, dexamethasone, panobinostat and pomalidomide were incubated with cells for 72 hours in the presence of Promega real-time Glo. The optimal concentrations and incubation times were inferred from this data, and used in measuring the response of IL6Myc cells to the pharmacological agents according to the following table:

Pharmacological agent	**Length of administration**	**Initial Concentration**	**Dilution Factor**
Bortezomib	24hr	1 μM	1:3
Melphalan	72hr	50 μM	1:2
4-Hydroperoxy Cyclophosphamide	72hr	10 μM	1:4
Dexamethasone	72hr	10 μM	1:3
Panobinostat	72hr	10 μM	1:3
Pomalidomide	72hr	10 μM	1:2

RNA Sequencing of IL6Myc Cell Lines: RNA was extracted using the RNeasy mini kit (Qiagen, 74106) from three technical replicates of each cell line. RNA quantity and quality was confirmed using the Thermofisher Nanodrop machine and 5300 Fragment Analyzer System (Agilent). Bioinformatics analysis of RNA sequencing data was conducted in R-Studio 4.1.1 and was done as follows. TrimGalore! was used to trim adapters of the RNA-seq library and then the data was mapped to GENCODE VM27 GTF file from the GRCm39 assembly with Salmon version 1.5.1. Differential expression testing was performed using the DESeq2 package which allowed extraction of TPM, FPKM, and RPKM data for downstream analysis. Figures were plotted using ggplot2 in R-Studio 4.1.1. Knitted R scripts are included as additional supplemental documents.

Statistical Analysis: All statistical analysis was conducted using RStudio and Graphpad Prism as described above.

Supplemental Tables:

Table S1. Top 100 Gene Sets Enriched in IL6Myc Tumor When Compared to Activated B Cell Control

Gene Set	Enrichment Score	Normalized Enrichment Score	Nominal P-Value	FDR q-value	FWER p-value
PASQUALUCCI_LYMPHOMA_BY_GC_STAGE_UP	0.54	3.06	0	0	0
PICCALUGA_ANGIOIMMUNOBLASTIC_LYMPHOMA_UP	0.51	2.74	0	0	0
NABA_ECM_REGULATORS	0.48	2.53	0	0	0
BOYLAN_MULTIPLE_MYELOMA_C_D_DN	0.45	2.52	0	0	0
REACTOME_EXTRACELLULAR_MATRIX_ORGANIZATION	0.45	2.51	0	0	0
KEGG_LYSOSOME	0.5	2.48	0	0	0
QI_PLASMACYTOMA_DN	0.52	2.47	0	0	0
DELPUECH_FOXO3_TARGETS_UP	0.57	2.44	0	0	0
KINSEY_TARGETS_OF_EWSR1_FLII_FUSION_DN	0.42	2.41	0	0	0.002
KOBAYASHI_EGFR_SIGNALING_24HR_UP	0.51	2.38	0	0	0.002
ZHENG_GLIOBLASTOMA_PLASTICITY_DN	0.57	2.33	0	0	0.003
KEGG_COMPLEMENT_AND_COAGULATION_CASCADES	0.56	2.33	0	0	0.003
LIU_PROSTATE_CANCER_DN	0.39	2.33	0	0	0.003
MORI_PLASMA_CELL_UP	0.55	2.32	0	0	0.004
PID_INTEGRIN1_PATHWAY	0.55	2.31	0	0	0.004
JAATINEN_HEMATOPOIETIC_STEM_CELL_DN	0.43	2.31	0	0	0.005
NABA_CORE_MATRISOME	0.43	2.3	0	0	0.005
REACTOME_COLLAGEN_FORMATION	0.52	2.3	0	0	0.005
REACTOME_IMMUNOREGULATORY_INTERACTIONS_BETWEEN_A_LYMPHOID_AND_A_NON_LYMPHOID_CELL	0.49	2.27	0	0	0.01
TAKEDA_TARGETS_OF_NUP98_HOXA9_FUSION_10D_DN	0.46	2.27	0	0	0.01
REACTOME_O_GLYCOSYLATION_OF_TSR_DOMAIN_CONTAINING_PROTEINS	0.61	2.27	0	0	0.011
BOYLAN_MULTIPLE_MYELOMA_PCA1_UP	0.46	2.27	0	0	0.011
REACTOME_INTEGRIN_CELL_SURFACE_INTERACTIONS	0.5	2.26	0	0.001	0.015
REACTOME_DEGRADATION_OF_THE_EXTRACELLULAR_MATRIX	0.47	2.26	0	0.001	0.016
PID_INTEGRIN_CS_PATHWAY	0.65	2.25	0	0.001	0.017
NABA_MATRISOME_ASSOCIATED	0.37	2.23	0	0.001	0.018
BAELDE_DIABETIC_NEPHROPATHY_UP	0.49	2.23	0	0.001	0.018
REACTOME_ASSEMBLY_OF_COLLAGEN_FIBRILS_AND_OTHER_MULTIMERIC_STRUCTURES	0.55	2.23	0	0.001	0.021
CHYLA_CBFA2T3_TARGETS_UP	0.38	2.21	0	0.001	0.029
WANG_IMMORTALIZED_BY_HOXA9_AND_MEIS1_UP	0.59	2.2	0	0.001	0.032
HOLLERN_MICROACINAR_BREAST_TUMOR_UP	0.56	2.19	0	0.001	0.034
REACTOME_DISEASES_ASSOCIATED_WITH_O_GLYCOSYLATION_OF_PROTEINS	0.53	2.19	0	0.001	0.035
BOQUEST_STEM_CELL_UP	0.4	2.17	0	0.001	0.049
CHARAFE_BREAST_CANCER_LUMINAL_VS_MESENCHYMAL_UP	0.37	2.17	0	0.001	0.049
BASSO_HAIRY_CELL_LEUKEMIA_UP	0.48	2.16	0	0.002	0.058

NABA_ECM_GLYCOPROTEINS	0.43	2.16	0	0.001	0.059
HESS_TARGETS_OF_HOXA9_AND_MEIS1_DN	0.46	2.15	0	0.001	0.059
REACTOME_IRE1ALPHA_ACTIVATES_CHAPERONES	0.5	2.14	0	0.002	0.076
REACTOME_GLYCOSPHINGOLIPID_METABOLISM	0.55	2.14	0	0.002	0.081
REN_ALVEOLAR_RHABDOMYOSARCOMA_DN	0.36	2.14	0	0.002	0.082
ZHAN_MULTIPLE_MYELOMA_MS_UP	0.54	2.13	0	0.002	0.089
MEBARKI_HCC_PROGENITOR_FZD8CRD_DN	0.38	2.13	0	0.002	0.091
HUANG_GATA2_TARGETS_UP	0.4	2.1	0	0.003	0.127
TURASHVILI_BREAST_DUCTAL_CARCINOMA _VS_DUCTAL_NORMAL_DN	0.41	2.1	0	0.003	0.127
REACTOME_SPHINGOLIPID_METABOLISM	0.46	2.1	0	0.003	0.129
KEGG_GLYCOSAMINOGLYCAN_DEGRADATION	0.68	2.1	0	0.003	0.131
REACTOME_REGULATION_OF_INSULIN_LIKE_ GROWTH_FACTOR_IGF_TRANSPORT_AND_ UPTAKE_BY_INSULIN_LIKE_GROWTH_FACTOR_ BINDING_PROTEINS_IGFBPS	0.45	2.1	0	0.003	0.131
SASAI_RESISTANCE_TO_NEOPLASTIC_ TRANSFROMATION	0.52	2.1	0	0.003	0.14
KORKOLA_YOLK_SAC_TUMOR	0.53	2.1	0	0.003	0.141
KEGG_CELL_ADHESION_MOLECULES_CAMS	0.43	2.09	0	0.003	0.151
WP_COMPLEMENT_AND_COAGULATION_CASCADES	0.51	2.09	0	0.003	0.155
REACTOME_SRP_DEPENDENT_COTRANSLATIONAL_ PROTEIN_TARGETING_TO_MEMBRANE	0.43	2.08	0	0.003	0.166
WP_PROSTAGLANDIN_SYNTHESIS_AND_REGULATION	0.54	2.08	0	0.003	0.166
APPEL_IMATINIB_RESPONSE	0.58	2.08	0	0.003	0.169
SMID_BREAST_CANCER_LUMINAL_A_UP	0.48	2.08	0	0.003	0.172
LIM_MAMMARY_STEM_CELL_UP	0.36	2.08	0	0.003	0.177
VART_KSHV_INFECTION_ANGIOGENIC_MARKERS_DN	0.43	2.08	0	0.003	0.185
REACTOME_COLLAGEN_BIOSYNTHESIS_ AND_MODIFYING_ENZYMES	0.5	2.08	0	0.003	0.186
TAKEDA_TARGETS_OF_NUP98_HOXA9_FUSION_8D_DN	0.4	2.08	0	0.003	0.186
REACTOME_PEPTIDE_LIGAND_BINDING_ RECEPTORS	0.43	2.07	0	0.003	0.188
ONDER_CDH1_TARGETS_2_UP	0.37	2.07	0	0.003	0.188
REACTOME_AMYLOID_FIBER_FORMATION	0.48	2.06	0	0.004	0.216
SIMBULAN_PARP1_TARGETS_UP	0.56	2.06	0	0.004	0.216
REACTOME_CLASS_A_1_RHODOPSIN_ LIKE_RECEPTORS	0.39	2.06	0	0.004	0.219
INGRAM_SHH_TARGETS_UP	0.42	2.05	0	0.004	0.227
VALK_AML_CLUSTER_8	0.61	2.05	0	0.004	0.249
CHYLA_CBFA2T3_TARGETS_DN	0.37	2.04	0	0.004	0.259
WP_GLYCOSAMINOGLYCAN_DEGRADATION	0.68	2.04	0	0.004	0.276
CASORELLI_APL_SECONDARY_VS_DE_NOVO_UP	0.52	2.04	0	0.004	0.28
HUANG_FOXA2_TARGETS_DN	0.56	2.04	0	0.004	0.286
AMIT_SERUM_RESPONSE_240_MCF10A	0.49	2.04	0	0.004	0.288
ANASTASSIOU_MULTICANCER_INVASIVENESS_ SIGNATURE	0.49	2.04	0	0.004	0.288
REACTOME_O_LINKED_GLYCOSYLATION	0.44	2.04	0	0.004	0.294
BROWNE_HCMV_INFECTION_16HR_DN	0.46	2.03	0	0.004	0.302

WINNEPENNINCKX_MELANOMA_METASTASIS_DN	0.53	2.03	0	0.005	0.314
WU_CELL_MIGRATION	0.39	2.03	0	0.005	0.323
TARTE_PLASMA_CELL_VS_B_LYMPHOCYTE_UP	0.44	2.02	0	0.005	0.331
SCHLINGEMANN_SKIN_CARCINOGENESIS_TPA_DN	0.58	2.02	0	0.005	0.335
REACTOME_BINDING_AND_UPTAKE_OF_ LIGANDS_BY_SCAVENGER_RECEPTORS	0.54	2.02	0	0.005	0.335
RAMALHO_STEMNESS_DN	0.44	2.02	0	0.005	0.342
MEISSNER_BRAIN_HCP_WITH_H3K4ME2_ AND_H3K27ME3	0.52	2.02	0	0.005	0.342
MAGRANGEAS_MULTIPLE_MYELOMA_ IGLL_VS_IGLK_DN	0.6	2.01	0	0.005	0.373
KEGG_SPHINGOLIPID_METABOLISM	0.53	2.01	0	0.005	0.373
CHIARADONNA_NEOPLASTIC_ TRANSFORMATION_KRAS_CDC25_DN	0.47	2.01	0	0.005	0.377
PETROVA_ENDOTHELIUM_LYMPHATIC_VS_BLOOD_DN	0.39	2.01	0	0.005	0.377
WEST_ADRENOCORTICAL_TUMOR_DN	0.34	2.01	0	0.005	0.382
STEARMAN_TUMOR_FIELD_EFFECT_UP	0.52	2.01	0.002	0.005	0.39
ONGUSAHA_TP53_TARGETS	0.51	2	0	0.005	0.397
FLORIO_NEOCORTEX_BASAL_RADIAL_GLIA_UP	0.37	2	0	0.005	0.411
GAUSSMANN_MLL_AF4_FUSION_TARGETS_F_UP	0.38	2	0	0.006	0.419
MCMURRAY_TP53_HRAS_COOPERATION_RESPONSE_DN	0.48	2	0	0.005	0.421
CHIARADONNA_NEOPLASTIC_TRANSFORMATION_KRAS_ DN	0.39	2	0	0.005	0.422
JAEGER_METASTASIS_DN	0.39	2	0	0.005	0.422
PIONTEK_PKD1_TARGETS_UP	0.54	1.99	0	0.006	0.449
LIAN_LIPA_TARGETS_6M	0.44	1.99	0	0.006	0.45
MARZEC_IL2_SIGNALING_DN	0.52	1.99	0	0.006	0.456
PID_INTEGRIN2_PATHWAY	0.58	1.99	0	0.006	0.456
REACTOME_MUSCLE_CONTRACTION	0.39	1.99	0	0.006	0.457
VALK_AML_CLUSTER_9	0.52	1.99	0	0.006	0.459
REACTOME_COMPLEMENT_CASCADE	0.52	1.99	0	0.006	0.462

Table S2. Genes found in >5 leading edges of gene sets found to be enriched by GSEA.

Gene Name	Number of Leading Edges Genes that Contain Gene
TGFBI	17
CLU	14
AQP3	14
CTSB	14
DUSP1	13
FBN1	13
LYZ	13
IGFBP6	13
FN1	12

SLPI	12
CD9	12
TIMP3	12
THBS1	12
MMP2	12
MMP9	12
EHF	12
FOS	11
RECK	11
NRP1	11
CDKN1A	11
GPNMB	11
DAB2	11
CEBPD	11
DCN	11
C3	11
COL1A1	11
COL1A2	11
EMP1	11
PCOLCE	11
COL5A1	11
SERPINF1	11
SPARC	11
C1S	10
EPAS1	10
LPAR1	10
APOE	10
TGM2	10
ACTA2	10
CFH	10
EPCAM	10
TPM1	10
AEBP1	10
KRT7	10
PPL	10
NT5E	10
POSTN	10
CD24	10
CDH1	10
RHOB	10
DPYSL3	9
C1R	9
LOXL2	9

CAV1	9
BTG2	9
CDH11	9
RBPMS	9
FHL1	9
FCGR2A	9
SPON1	9
ID2	9
LAMC2	9
IRF6	9
PDLIM4	9
DKK3	9
ST14	9
AXL	9
COL4A1	9
SELENOP	9
TXNIP	8
GSTM1	8
COL3A1	8
LY6E	8
TNFRSF21	8
PDCD4	8
ANPEP	8
CRISPLD2	8
ARHGEF3	8
PLAT	8
ENPP2	8
MANSC1	8
SNAI2	8
TIMP2	8
FGL2	8
VAV3	8
C1QB	8
C1QA	8
CP	8
EMP3	8
FSTL1	8
MAF	8
S100A4	8
CXCL12	8
TP53INP1	8
CCN5	8
CTSS	8

CAVIN1	8
CALD1	8
VCAN	8
METTL7A	8
IGFBP7	8
CDO1	8
MTUS1	8
ITM2A	8
TSC22D3	8
SGK1	8
MPZL2	8
COL4A2	8
NID1	8
PTGIS	8
CXADR	7
PDGFC	7
NR2F2	7
ITGB5	7
ITGB4	7
ARL4C	7
LGALS1	7
MT1F	7
KCTD12	7
AKAP12	7
IL18	7
KIT	7
TMEM176B	7
TMEM176A	7
PLAU	7
PPIC	7
HTRA1	7
RARRES2	7
TNFAIP2	7
TENT5C	7
COL7A1	7
CFB	7
HMOX1	7
TIMP1	7
GAS6	7
GRN	7
PAPSS2	7
TPM2	7
COL14A1	7

MAGED1	7
PARVA	7
TMED3	7
LSR	7
PID1	7
CLDN7	7
MYL9	7
SAT1	7
S100A9	7
S100A8	7
ENTPD1	7
TM4SF1	7
CCND1	7
INHBB	7
MMP8	7
LAMB2	7
DAPK1	7
FZD2	7
TGFB1I1	7
ENG	7
MITF	7
RHOBTB3	7
KLF4	7
APP	7
GLUL	7
TNS1	7
IGSF6	7
BASP1	7
SIRPA	7
C5AR1	7
LTBP2	7
MYH11	7
SPINT2	6
PLA2G7	6
JUP	6
PBX1	6
SLCO3A1	6
CRLF1	6
FADS3	6
IL6ST	6
FTL	6
TNFRSF1A	6
ITGA5	6

GZMA	6
TSPAN13	6
ICAM2	6
LGALS3	6
MT2A	6
TGFA	6
MSR1	6
MYO5C	6
SDC1	6
ECHDC2	6
DDR1	6
DDR2	6
ENPP1	6
SCNN1A	6
VCAM1	6
MXD4	6
TNFAIP6	6
CLEC10A	6
GJA1	6
GNS	6
LDHB	6
ELL2	6
PAM	6
COPZ2	6
ALOX5	6
SQOR	6
FOSB	6
RAB25	6
IFITM3	6
NBL1	6
CST3	6
QPCT	6
F2RL1	6
C1QC	6
LPL	6
FBLN1	6
BLNK	6
ALDH1A3	6
COL6A2	6
THBS2	6
SNCA	6
LUM	6
MYLK	6

RNASE4	6
HSD11B1	6
P2RY14	6
PLXDC1	6
RORA	6
S100A6	6
RGCC	6
CCL2	6
QSOX1	6
CTTN	6
CD59	6
RAMP1	6
FHOD3	6
NDRG2	6
TMEM45A	6
RBM47	6
MAPK13	6
ABAT	6
MYB	6
MEG3	6
SERPINH1	6
FZD1	6
SSPN	6
PRSS23	6
ANXA1	6
ANXA2	6
ANXA3	6
ANXA5	6
PAWR	6
CCL23	6
IGFBP4	6
IGFBP3	6
F2R	6
MAFB	6
CLEC3B	6
AHNAK2	6
TRAM2	6
GLIPR1	6
CEACAM1	6
TFEC	6
TGFB2	6
ARHGAP29	6
SMAD6	6

DOCK4	6
ABCC3	6
HPGD	6
ALOX5AP	6
PMP22	6

Table S3. Summary of gene fusions in IL6Myc

Fusion Name	Junction Read Count	Spanning Fragment Count	Left Breakpoint	Right Breakpoint	FFPM	Fusion Partners found in Human MM
Igkv8-28--Igkc	1	16589	chr6:70144113:-	chr6:70726435:+	667.6718	N/A
Igkv8-27--Igkc	25	10574	chr6:70172042:-	chr6:70726435:+	414.4741	N/A
Igkv14-111--Igkc	4	9619	chr6:68256458:+	chr6:70726478:+	323.8263	N/A
Ighv1-47--Ighg2c	9	6090	chr12:114991489:-	chr12:113288932:-	245.4569	N/A
Igkv4-72--Igkc	16	5269	chr6:69227056:-	chr6:70726478:+	163.5317	N/A
Igkv14-111--Igkc	36	4711	chr6:68256458:+	chr6:70726435:+	155.5354	N/A
Igkv14-111--Igkc	5	4711	chr6:68256614:+	chr6:70726478:+	154.5197	N/A
Igkv14-111--Igkc	21	2549	chr6:68256458:+	chr6:70726435:+	101.6509	N/A
Igkv14-111--Igkc	4	2549	chr6:68256458:+	chr6:70726478:+	100.9785	N/A
Igkv14-111--Igkc	3	2549	chr6:68256614:+	chr6:70726478:+	100.939	N/A
Igkv14-111--Igha	3	2410	chr6:68256658:+	chr12:113259069:-	81.2006	N/A
Igha--Igkc	3	1714	chr12:113259084:-	chr6:70726576:+	61.1019	N/A
Igkv5-39--Igkc	1	1042	chr6:69900929:-	chr6:70726435:+	37.1166	N/A
Ighv9-3--Ighg1	5	611	chr12:114140922:-	chr12:113330523:-	20.1832	N/A
Igkc--Igkv8-28	4	473	chr6:70726858:+	chr6:70144175:-	19.1971	N/A
Ighv1-47--Igkv8-28	4	459	chr12:114991206:-	chr6:70144165:-	18.6337	N/A
Igkv8-27--Ighg1	1	438	chr6:70172222:-	chr12:113329882:-	17.1671	N/A
Igkv5-43--Igkc	1	505	chr6:69823863:-	chr6:70726435:+	16.665	N/A
Slpi--Ighg1	1	371	chr2:164356188:-	chr12:113330523:-	12.1886	None
Igha--Igkv3-5	1	308	chr12:113259934:-	chr6:70663586:+	10.9906	N/A
Igkv4-77--Igkc	8	240	chr6:69111106:-	chr6:70726435:+	9.9809	N/A
Ighv3-6--Igha	6	143	chr12:114288540:-	chr12:113260236:-	5.3883	N/A
Igkv1-135--Igkc	5	128	chr6:67609793:+	chr6:70726435:+	4.3804	N/A
Igkv6-23--Igkc	1	85	chr6:70260885:-	chr6:70726435:+	2.8324	N/A
Igkv14-111--Igkc	1	86	chr6:68256458:+	chr6:70726435:+	2.6899	N/A
Igkv14-111--Igkc	2	75	chr6:68256458:+	chr6:70726435:+	2.6229	N/A

Igkv1-135--Igkc	5	51	chr6:67609793:+	chr6:70726435:+	2.1345	N/A
Igkv1-135--Igkc	1	61	chr6:67609793:+	chr6:70726435:+	1.917	N/A
Igkv1-88--Igkc	1	52	chr6:68862983:-	chr6:70726435:+	1.7455	N/A
Igkv10-96--Igkc	2	49	chr6:68632382:-	chr6:70726435:+	1.7372	N/A
Igkv5-45--Igkc	39	11	chr6:69776258:-	chr6:70726435:+	1.7032	N/A
Igkv10-96--Igkc	1	43	chr6:68632382:-	chr6:70726435:+	1.6771	N/A
Igkv1-135--Igkc	4	39	chr6:67609793:+	chr6:70726435:+	1.4648	N/A
Igkv6-17--Igkc	1	43	chr6:70371517:+	chr6:70726435:+	1.3604	N/A
Igkv1-135--Igkc	6	23	chr6:67609793:+	chr6:70726435:+	1.147	N/A
Igkv1-135--Igkc	2	27	chr6:67609793:+	chr6:70726435:+	1.0382	N/A
Igkv17-121--Igkc	1	27	chr6:68036872:+	chr6:70726435:+	0.9538	N/A
Gm4242--Igha	22	0	chr19:61232417:-	chr12:113260236:-	0.7829	None
Igkv14-111--Igkc	1	19	chr6:68256458:+	chr6:70726435:+	0.7623	N/A
Rpl4--Ighg1	1	18	chr9:64176216:+	chr12:113329298:-	0.7516	RPL4
Igkv2-109--Igkc	4	14	chr6:68302932:+	chr6:70726435:+	0.6861	N/A
Igkv5-39--Igkc	1	16	chr6:69900929:-	chr6:70726435:+	0.648	N/A
Igkv12-46--Igkc	4	13	chr6:69764944:-	chr6:70726435:+	0.5791	N/A
Igkv12-46--Igkc	1	17	chr6:69764944:-	chr6:70726435:+	0.5565	N/A
Ifi204--Ifi202b	14	0	chr1:173766811:-	chr1:173982741:-	0.4332	None
Igkv9-124--Igkc	1	10	chr6:67942486:-	chr6:70726435:+	0.4193	N/A
Gm43218--Igkc	1	11	chr6:70240924:-	chr6:70726435:+	0.3952	None
Cd74--Igkv8-27	1	9	chr18:60808077:+	chr6:70172270:-	0.391	CD74
Gm42543--Igkc	9	2	chr6:68880620:-	chr6:70726435:+	0.3747	None
Igkv9-120--Igkc	1	9	chr6:68050037:+	chr6:70726435:+	0.358	N/A
Igkv2-109--Igkc	4	6	chr6:68302932:+	chr6:70726435:+	0.3092	N/A
Ifi204--Ifi202b	8	0	chr1:173766811:-	chr1:173982741:-	0.2845	None
Ighg1--Atp5b	1	6	chr12:113330233:-	chr10:128085442:+	0.2769	None
Igkv2-109--Igkc	3	4	chr6:68302927:+	chr6:70726435:+	0.2506	N/A
Sept1--Igha	2	5	chr7:127215868:-	chr12:113259162:-	0.2491	None
Igkv12-98--Igkc	1	6	chr6:68570811:+	chr6:70726435:+	0.2385	N/A
Igkv12-98--Igkc	1	5	chr6:68570811:+	chr6:70726435:+	0.1976	N/A
Gm42047--Ly6e	5	0	chr8:121841186:+	chr15:74957777:+	0.1779	LY6E
Hnrnpu--Slpi	1	3	chr1:178333547:-	chr2:164354313:-	0.1609	HNRNPU
Ighv14-4--Ighm	1	3	chr12:114176822:-	chr12:113422730:-	0.1524	N/A

Snd1--Braf	3	1	chr6:28545598:+	chr6:39648486:-	0.1423	**Both/Same Fusion Partners**
Tbc1d10c--H2-Ea-ps	4	0	chr19:4188944:-	chr17:34342295:-	0.1363	TBC1D1
Igkv9-129--Igkc	2	2	chr6:67839847:+	chr6:70726435:+	0.1362	N/A
Gm47283--Taf6l	4	0	chrY:90785719:+	chr19:8778925:-	0.1238	None
mt-Nd5--Cotl1	3	1	chrM:12641:+	chr8:119809884:-	0.1237	None
Eef2--Rack1	3	0	chr10:81182082:+	chr11:48805585:+	0.1207	EEF2
Zfp784--Syvn1	3	0	chr7:5035076:-	chr19:6051207:+	0.1207	SYVN1
Ighv1-47--Dhx9	1	2	chr12:114991489:-	chr1:153464712:-	0.1207	DHX9
Ighv1-47--Irf3	1	2	chr12:114991489:-	chr7:45000645:+	0.1207	IRF3
Cerk--Apoe	3	0	chr15:86140752:-	chr7:19696526:-	0.1187	None
Cst3--Akap8l	3	0	chr2:148875171:-	chr17:32332892:-	0.1187	None
F13a1--Macf1	3	0	chr13:36892818:-	chr4:123351015:-	0.1187	MACF1
Foxk1--Cd74	3	0	chr5:142458486:+	chr18:60803923:+	0.1187	Both/Different Fusion Partners
Ifi204--Ifi202b	3	0	chr1:173766811:-	chr1:173982741:-	0.1187	None
Paip2b--Fcrl1	3	0	chr6:83809963:-	chr3:87384759:+	0.1187	None
Rpl23a--Igkv8-27	1	2	chr11:78182803:-	chr6:70172270:-	0.1173	RPL23A
Gm21887--Mid1	3	0	chrX:170018795:+	chrX:169966063:+	0.1143	None
H2-Eb1--Cd37	3	0	chr17:34314451:+	chr7:45233978:-	0.1143	CD37
Cd22--Cd37	1	2	chr7:30869510:-	chr7:45233978:-	0.1143	CD37
Igkv12-98--Igkc	1	2	chr6:68570811:+	chr6:70726435:+	0.1143	N/A
Igkv4-92--Igkc	1	2	chr6:68755545:-	chr6:70726435:+	0.1143	N/A
Trmt1--Usp32	1	2	chr8:84698293:+	chr11:85022307:-	0.1143	None
Arhgap15--Psmc1	3	0	chr2:44386737:+	chr12:100114892:+	0.1074	None
Polm--Rbm25	3	0	chr11:5837319:-	chr12:83668219:+	0.1074	RBM25rn
Tab3--Ikzf1	3	0	chrX:85574165:+	chr11:11700205:+	0.1074	None
Gm21887--Mid1	1	2	chrX:170018795:+	chrX:169985936:+	0.1074	None
Hvcn1--H2-Ea-ps	1	2	chr5:122216363:+	chr17:34342295:-	0.1074	None
Cep170--Strap	3	0	chr1:176739969:-	chr6:137745608:+	0.1068	None
Birc6--Cdk12	3	0	chr17:74662818:+	chr11:98263470:+	0.1022	Both/Different Fusion Partners
Slc9a7--Chst7	3	0	chrX:20105921:-	chrX:20096965:+	0.1022	None
Txnip--H2-Ea-ps	1	2	chr3:96559217:+	chr17:34342295:-	0.1022	TXNIP
Upf2--Ylpm1	3	0	chr2:6010428:+	chr12:85064971:+	0.101	YLPM1

Table S4. Summary of genes with multiple variants in IL6Myc tumors

Gene	Freq
Myc	26
Ttn	6
Cntnap4	5
Lrp1b	5
Ccdc163	4
Flg2	4
Hist1h1c	4
Lrrc63	4
Pcbp1	4
Pim1	4
Setd3	4
Unc13d	4
Csmd3	3
Fancm	3
Hist1h1d	3
Hnrnpa2b1	3
Nav3	3
Nbea	3
Pclo	3
Prh1	3
Rptn	3
Sfr1	3
Spink5	3
Stat2	3
Strn	3
Wtip	3
2010300C02Rik	2
4931408C20Rik	2
4932429P05Rik	2
4932438A13Rik	2
4933408B17Rik	2
9530068E07Rik	2
A1cf	2
Acss2	2
Arhgap28	2
Atp5c1	2
BC049635	2
Bc1,Elane	2
Ccdc115	2

Ccdc144b	2
Ccdc151	2
Cd83	2
Cebpz	2
Chodl	2
Cntfr	2
Crym	2
Csmd1	2
Dapk1	2
Dlgap4	2
Dmd	2
Dnah2	2
Eif4a2	2
Eif5	2
Eif5a	2
Epn2	2
EU599041	2
Evpl	2
Ezh2	2
Fam173b	2
Fam5c	2
Fat1	2
Fat2	2
Fat4	2
Fbxo30	2
Fign	2
Fndc1	2
Gm5506	2
Prpmp5	2
Gpi1	2
Gpr98	2
Hils1	2
Hist1h1e	2
Hist1h2ag	2
Hist1h2ai	2
Hist1h2bc	2
Huwe1	2
Il4i1	2
Itpr1	2
Jarid2	2

Kars	2
Katnal1	2
Krt78	2
Krtap5-3	2
Lhx3	2
Lnp	2
Lrriq1	2
Magi1	2
Map3k19	2
Morc4	2
Msh6	2
Muc5ac	2
Myo15	2
Myo18b	2
Nedd4	2
Neil1	2
Nfatc2ip	2
Nhsl2	2
Nono	2
Oasl2	2
Olfr1189	2
Pcdh9	2
Pkd1l3	2
Pkhd1l1	2
Plod2	2
Pls1	2
Prdm9	2
Prp2	2
Prss36	2
Rassf9	2
Rp1l1	2
Rpl8	2
Rplp1	2
Rps3a1	2
Sash1	2
Selplg	2
Sfswap	2
Sipa1l3	2
Six3os1	2
Skap1	2

Slfn14	2
Smarca4	2
Son	2
Srsf6	2
Stard8	2
Sycp1	2
Tacc3	2
Thoc1	2
Tmpo	2
Tmx3	2
Tpi1	2
Tro	2
Ttc14	2
Ttc37	2
Ttf1	2
Ush2a	2
Usp19	2
Vmn1r196	2
Vps13c	2
Xirp2	2
Ylpm1	2
Zan	2
Zfp747	2
Zfp780b	2

Table S5. Overlaping gene sets found in IL6Myc primary tumor and IL6Myc cell lines when compared to activated B cells.

Gene Set	Rank in Primary Tumor	Rank in Cell Line
BOYLAN_MULTIPLE_MYELOMA_C_D_DN	3	6
QI_PLASMACYTOMA_DN	5	3
FOROUTAN_TGFB_EMT_DN	6	70
FOROUTAN_INTEGRATED_TGFB_EMT_DN	10	49
TAKEDA_TARGETS_OF_NUP98_HOXA9_FUSION_10D_DN	12	68
MORI_PLASMA_CELL_UP	13	38
BAELDE_DIABETIC_NEPHROPATHY_UP	15	62
BOYLAN_MULTIPLE_MYELOMA_PCA1_UP	16	12
APPEL_IMATINIB_RESPONSE	19	29
SASAI_RESISTANCE_TO_NEOPLASTIC_TRANSFROMATION	30	59
CHYLA_CBFA2T3_TARGETS_DN	49	33

FOSTER_KDM1A_TARGETS_UP	50	30
TARTE_PLASMA_CELL_VS_B_LYMPHOCYTE_UP	55	10
BLANCO_MELO_RESPIRATORY_SYNCYTIAL_VIRUS_INFECTION_A594_CELLS_DN	59	46
KIM_RESPONSE_TO_TSA_AND_DECITABINE_UP	65	90
SEAVEY_EPITHELIOID_HEMANGIOENDOTHELIOMA	66	73
MIKKELSEN_MEF_HCP_WITH_H3K27ME3	99	35

Supplement References

1. Subramanian, A., Tamayo, P., Mootha, V. K., et al. (2005). Gene set enrichment analysis: a knowledge-based approach for interpreting genome-wide expression profiles. Proc. Natl. Acad. Sci. U.S.A. 102, 15545–15550.

2. Korotkevich G, Sukhov V, Sergushichev A (2019). Fast gene set enrichment analysis. bioRxiv. doi: 10.1101/060012, http://biorxiv.org/content/early/2016/06/20/060012.

3. Liberzon A, Birger C, Thorvaldsdóttir H, Ghandi M, Mesirov JP, Tamayo P. The Molecular Signatures Database (MSigDB) hallmark gene set collection. Cell Syst. 2015;1(6):417-425

4. Foltz SM, Gao Q, Yoon CJ, et al. Evolution and structure of clinically relevant gene fusions in multiple myeloma. Nat Commun. 2020;11(1):2666.

5. Cibulskis K, Lawrence MS, Carter SL, et al. Sensitive detection of somatic point mutations in impure and heterogeneous cancer samples. Nat Biotechnol. 2013;31(3):213-9.

6. McLaren W, Gil L, Hunt SE, et al. The Ensembl Variant Effect Predictor. Genome Biol. 2016;17(1):122.